Received: 28 August 2021 | Revised: 30 November 2021 | Accepted: 9 December 2021

DOI: 10.1111/jfpe.13958

ORIGINAL ARTICLE

Journal of Food Process Engineering WILEY

Transient computer simulation of the temperature profile in different packaging materials: An optimization of thermal treatment of tender coconut water

V. Prithviraj[1] | Ravi Pandiselvam[2] | M. R. Manikantan[2] | S. V. Ramesh[2] | P. P. Shameena Beegum[2] | Anjineyulu Kothakota[3] | Amin Mousavi Khaneghah[4]

[1]Department of Food Engineering, National Institute of Food Technology Entrepreneurship and Management, Sonipat, India

[2]Physiology, Biochemistry, and Post-Harvest Technology Division, ICAR–Central Plantation Crops Research Institute, Kasaragod, Kerala, India

[3]Agro-Processing and Technology Division, CSIR-National Institute for Interdisciplinary Science and Technology (NIIST), Trivandrum, Kerala, India

[4]Department of Food Science and Nutrition, Faculty of Food Engineering, University of Campinas (UNICAMP), Campinas, Sao Paulo, Brazil

Correspondence
Ravi Pandiselvam and M. R. Manikantan, Physiology, Biochemistry, and Post-Harvest Technology Division, ICAR–Central Plantation Crops Research Institute, Kasaragod 671124, Kerala, India.
Email: anbupandi1989@yahoo.co.in and manicpcri@gmail.com

Funding information
Indian Council of Agricultural Research (ICAR)-All India Coordinated Research Project on Post-Harvest Engineering & Technology (AICRP on PHET)

Abstract

Understanding the temperature profile of different packaging materials would be useful for selecting appropriate packaging material for in-bottle pasteurization. The temperature profile of polypropylene, polyethylene (PE), and polyethylene terephthalate bottles was investigated using COMSOL Multiphysics software to understand the temperature–time correlation with thermal treatments. PE bottles exhibited the least temperature difference between cold and hot spots. Optimization of thermal treatment processing parameters such as temperature (80–95°C) and treatment time (5–15 min) for inactivation of enzymes, namely polyphenol oxidase (PPO) and peroxidase (POD), in tender coconut water (TCW) was performed to the extent its shelf life. The quality parameters of heat-treated TCW such as pH, total soluble solids (TSS), titratable acidity (TA), turbidity, phenolic content, PPO, POD, and sensory evaluation were analyzed. The multiple linear regression models were developed for each quality parameter using a central composite design (CCD). The optimized treatment conditions were 84°C temperature and 5 min treatment time with the desirability of 0.926. The responses recorded were pH = 5.4, TSS = 5.52, turbidity = 7.1 NTU, TA = 0.06% of malic acid, relative PPO = 0.099, relative POD = 0.093, phenolic content = 44.712 mg gallic acid equivalent/L, and overall acceptability score = 8.

Practical Applications

Understanding the temperature profile of different packaging materials during pasteurization or sterilization is imperative to select the suitable packaging material, and also it would be helpful for designing the heating system. Tender coconut water (TCW) is the most popular natural drink in Asian countries. However, the pasteurization conditions are yet to be optimized to preserve TCW without affecting its bioactive and functional components. The current practice followed for in-bottle sterilization of TCW is polyethylene terephthalate (PET). This is due to PET being cheaper and readily available than

V. Prithviraj and Ravi Pandiselvam contributed equally and shared the first authorship.

other packaging materials. However, the quality of the TCW could affect PET due to improper heat distribution which can lead to damage of bioactive components. The present study has optimized the suitable pasteurization conditions and packaging material for bottling and marketing TCW. The findings of the present study will boost the market potential of the tender coconut processing industries.

1 | INTRODUCTION

The advancements in health, nutritional, and allied sectors worldwide have extensively promoted the demand for natural, nutritive, and healthy products such as tender coconut water (TCW). The liquid endosperm is also known as TCW, which remains inside the enclosure of external skin, husk, shell, and solid kernel, otherwise referred to as exocarp, mesocarp, endocarp, and endosperm, respectively (Pandiselvam et al., 2020).

TCW is a natural beverage having numerous health benefits. It can prevent various diseases (Campbell-Falck, Thomas, Falck, Tutuo, & Clem, 2000; Tan, Cheng, Bhat, Rusul, & Easa, 2014) and is loaded with an abundant source of protein and minerals (Camargo Prado et al., 2015; Segura-Badilla et al., 2020; Tan, Cheng, Bhat, Rusul, & Mat Easa, 2015). However, the high perishable nature of TCW, extraction, storage, and further value addition are significant challenges. It has been reported that the removal of husk and shell from TCW leads to qualitative degradation. Even though it is possible to keep the whole tender coconut fresh for 1 week, the transportation and marketing of the whole nut are cumbersome due to its bulky nature.

Nonthermal technologies such as ultrasound (Rajashri, Roopa, Negi, & Rastogi, 2020) and high-pressure processing (HPP) (Ma et al., 2019) have been evaluated to extend the shelf life of TCW, but their commercial application and economic feasibility remain a significant challenge. Also, some nonthermal techniques, including HPP, require heat treatment as preprocessing to inactivate TCW enzymes (Ma et al., 2019). Currently, most TCW processing industries are using unoptimized thermal treatment and preservatives for processing and storage. Hence, the treatment conditions require optimization to avoid the losses of heat-sensitive biochemical compounds.

A significant impediment in TCW processing is finding appropriate conditions for the inactivation of polyphenol oxidase (PPO) and peroxidase (POD) enzymes. These enzymes are causing a browning reaction in TCW (Nokthai, Lee, & Shank, 2010). The browning reaction causes the appearance of a pink tint in TCW, which ultimately affects the product's sensory properties. Besides, off-flavor development was also observed during the enzymatic reaction (Matsui, Granado, de Oliveira, & Tadini, 2007; Vamos-Vigyázó, 1981). However, the pink color formation can be controlled by developing suitable postharvest conservation and thermal processing technique (Cunha et al., 2020). In addition, untreated TCW will easily undergo fermentation reactions within 6–8 hr, and cause an increase in ethanol content and decrease in the sugar content (Olufunmi, Daniel, & Efem, 2020).

Thermal treatments are usually defined by temperature and time combinations. Nevertheless, while scaling up the laboratory treatments to an industrial scale application, the treatment combinations may not perform as expected, especially in final product quality. This is majorly due to the differences in uniformity of heat distribution during the process of upscaling. Although many researchers have suggested various temperature (80–130°C) and time (8–900 s) combinations for the treatment of TCW, the results obtained are inconsistent (Naik, Sunil, Rawson, & Venkatachalapathy, 2020). Hence, it is imperative to study the heating distribution behavior of packaging material used to process TCW to reproduce the results even at an industrial scale. However, the study on temperature distribution patterns in different packaging materials is scarce.

In this context, this study aimed to simulate the temperature profile of different packaging materials (PP, PE, and PET) commonly used for TCW bottling and optimize the thermal treatment condition suitable for the preservation of TCW using a central composite design.

2 | MATERIALS AND METHODS

2.1 | Temperature distribution profile

Computer simulations of packaging materials are replicated STEP (Standard for the Exchange of Product Data) files using Siemens Solid Edge 2019 software (Figure 1a). The simulation work was carried out using COMSOL Multiphysics 5.5.0.359 software with laminar flow interface and heat transfer in solids and fluids physics. Also, the geometry was analyzed with tetrahedron mesh with element size defaulting to normal.

A time-dependent study was initiated for 15 min by replicating the experimental conditions. Energy conservation equations for energy balance in solids (Equation 1) and fluids (Equation 2) were used as governing equations. Fluid behavior was modeled by following Navier–Stokes equations (Equations 4 and 5) simultaneously accounted during simulation.

$$\varrho C_p \frac{\partial T}{\partial t} + \varrho C_p u \times \nabla T + \nabla \times q = Q + Q_{\text{ted}}, \quad (1)$$

$$\varrho C_p \frac{\partial T}{\partial t} + \varrho C_p u \times \nabla T + \nabla \times q = Q + Q_p + Q_{\text{vd}}, \quad (2)$$

$$q = -kT \quad (3)$$

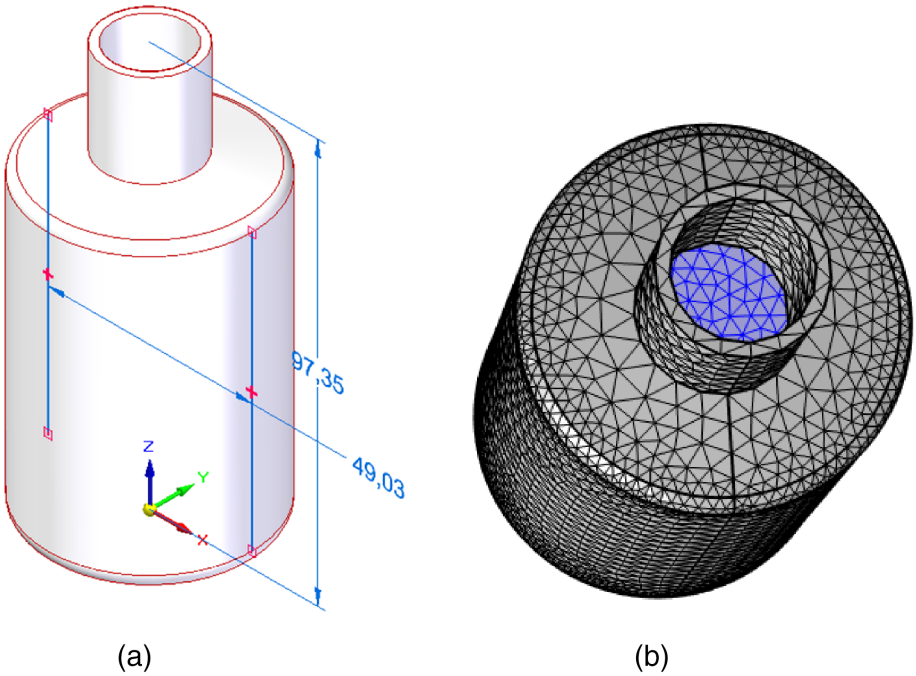

FIGURE 1 (a) STEP model of the bottle. (b) Meshed model of bottle

$$\varrho\frac{\partial u}{\partial t}+\varrho(u\times\nabla)u=\nabla\times[-\varrho I+K]+F+\varrho g, \tag{4}$$

$$\frac{\partial \varrho}{\partial t}+\nabla\times(\varrho u)=0. \tag{5}$$

where

ϱ = density
C_p = constant pressure heat capacity
T = temperature
t = time
u = fluid velocity vector
q = conductive heat flux
k = heat conductivity
Q = heat source
Q_{ted} = thermoelastic damping
Q_p = pressure work
Q_{vd} = viscous dissipation
F = volume force vector
g = acceleration due to gravity

The simulations were performed using different packaging bottles such as PP, PE, and PET with the same geometry. First, packaging bottles with water temperatures were set at 25°C, and heating source (water bath) temperature was set at 90°C as initial conditions. Then, a nonisothermal flow study was initiated with normal mesh size, as shown in Figure 1b.

2.2 | Raw materials

Tender coconuts of the variety West Coast Tall (WCT) of 6–7 months maturity was obtained from ICAR-Central Plantation Crops Research Institute (ICAR-CPCRI) Farm Section, Kasaragod, India. The nuts were taken to the Agro-Processing Centre immediately after harvest, and the TCW was extracted using Punch and Cutter developed by ICAR-CPCRI (Pandiselvam, Manikantan, Sunoj, Sreejith, & Beegum, 2019). TCW was pooled together and filtered using a 700-μm sieve to remove the coarse impurities. Stainless steel containers kept under deep freezer conditions (−18°C) were used to preserve TCW before the treatment. Afterward, these containers were kept outside to defreeze, which took 15–20 min to equilibrate with ambient conditions (29 ± 2°C and 62% RH). The TCW was filled in PE bottles (125 ml, 2 mm thick, Parsons Pvt. Ltd.) up to 100 ml before treatment. The PET bottles were selected for the heat treatment because of the more uniform temperature distribution.

2.3 | Heat treatment

A Rivotek PID-controlled digital display water bath shaker was used for imposing the heat treatment (maximum temperature of 100°C and ±0.1 accuracy). The TCW-filled PE bottles were kept in the water bath for different heat treatments, as mentioned in Table 1.

2.4 | Determination of quality parameters

The following quality parameters were analyzed after the heat treatment. All the experiments were replicated three times.

2.5 | pH, total soluble solids, and turbidity

pH was measured using a handheld pH meter (Testr35, Eutech Instruments, Paisley, United Kingdom), having 0.1 accuracies. Similarly, a

TABLE 1 Central composite design adopted for the heat treatment of tender coconut water

Independent variables		Dependent variables							
Temperature (°C)	Time (min)	pH	TSS (°Brix)	Turbidity (NTU)	Titratable acidity (% of malic acid)	Relative PPO (%)	Relative POD (%)	Phenolic content (mg of GAE/L)	Overall acceptability
87.5	10	5.43	5.44	7.505	0.0579	0.0000	0.0222	44.24	7.3333
95.0	15	5.56	5.60	9.246	0.0574	0.0000	0.0000	38.64	4.3333
80.0	15	5.55	5.47	6.853	0.0593	0.5555	0.3888	43.26	7.1667
87.5	10	5.43	5.45	7.658	0.0585	0.0000	0.0222	44.44	7.3100
95.0	5	5.55	5.55	6.953	0.0576	0.0000	0.0000	40.79	5.1667
87.5	5	5.54	5.43	7.203	0.0589	0.0555	0.1111	44.27	7.5000
87.5	15	5.53	5.55	7.930	0.0580	0.0000	0.0056	41.78	7.0000
80.0	5	5.50	5.43	6.173	0.0617	0.8889	0.7222	44.42	7.8333
87.5	10	5.43	5.46	7.562	0.0588	0.0000	0.0222	44.98	7.3800
80.0	10	5.57	5.50	6.496	0.0600	0.6667	0.5556	43.76	7.6667
95.0	10	5.56	5.57	8.283	0.0578	0.0000	0.0000	39.80	4.8333

Abbreviations: GAE, gallic acid equivalent; POD: peroxidase; PPO, polyphenol oxidase.

pocket refractometer (PAL-BX/RI-ATAGO CO., Ltd., Japan) was used to measure total soluble solids in °Brix with ±0.1 accuracy. Also, NTU measured turbidity using a turbidimeter (Eutech TN-100, Paisley, United Kingdom) having ±1 accuracy.

2.6 | Titratable acidity

Titratable acidity (TA) was examined by the method described by Thimmaiah (1999). The malic acid was the predominant acid in TCW (Yong, Ge, Ng, & Tan, 2009); hence, TA was expressed as mass of malic acid equivalent in 100 ml.

2.7 | Phenolic content

The phenolic content determination was carried out using the Folin–Ciocalteu method (Singleton, Orthofer, & Lamuela-Raventós, 1999) with slight modifications. Gallic acid was used for the preparation of a standard stock solution of 100 ppm concentration. A standard curve was obtained with a concentration range of 10–50 ppm. TCW sample of 0.1 ml was taken and diluted nine times using distilled water. Later, 0.2 ml of 50% Folic-Ciocalteu Reagent (FCR) and 2 ml of 7% Na_2CO_3 were added, vortexed, and incubated in the dark for 1 hr at room temperature (29 ± 2°C and 62% RH). Spectrophotometric absorbance was recorded using a Shimadzu UV-160 spectrophotometer at 750 nm, and results were expressed as in milligrams gallic acid equivalent (GAE)/L.

2.8 | PPO activity

PPO activity was determined according to the method described by Porto et al. (2020) with slight modifications. The TCW sample (1 ml) was added with potassium phosphate buffer (1 ml, pH = 6) containing catechol (0.1 M). Absorbance readings were measured using a spectrophotometer (Shimadzu UV-160) at 425 nm for every 15 s up to 30 min at room temperature. The enzymatic activity was calculated using Equation (6). PPO activity was expressed as a change in absorbance per minute.

$$\text{PPO activity}(\text{change in absorbance}/\text{min}) = \frac{k}{0.001}, \quad (6)$$

where k = slop of the absorbance versus time plot.

2.9 | POD activity

POD enzymatic activity was determined according to the method described by Porto et al. (2020) with slight modifications. A treated TCW sample of 1 ml was added with 950 µL of phosphate–citrate buffer (pH = 5) with 1% pyrogallol and 50 µL of 3% H_2O_2. The absorbance readings were measured using a spectrophotometer (Shimadzu UV-160) at 470 nm every 15 s up to 5 min at room temperature. The enzymatic activity was calculated using Equation (7). POD activity was expressed as absorbance change per minute.

$$\text{PPD Activity}(\text{Change in absorbance}/\text{min}) = \frac{k}{0.001}, \quad (7)$$

where k = slope of the absorbance versus time plot.

2.10 | Sensory evaluation

The sensory analysis was conducted according to the procedure of Mosqueda-Melgar, Raybaudi-Massilia, and Martín-Belloso (2012) and Pravitha, Manikantan, Kumar, Beegum, and Pandiselvam (2021). Briefly, a panel of eight trained persons (four males and four

females) from the age group of 20–55 years was selected for the sensory evaluation of treated samples. The scores were assigned in a 9-point Hedonic scale based on various factors: color, fermentation, aroma, freshness, off-flavor, sweetness, burnt feel, and overall acceptability (OA). The panelists were trained before starting the evaluation by definition of each sensory attribute. Fifteen milliliters of each sample were served into a cup, and a glass containing potable water was provided to panelists to eliminate the residual taste between samples. The overall acceptability factor was used in the response surface model. The samples were named starting from S1, which corresponds to 80°C and 5 min treatment, S2 with 80°C and 10 min treatment, till S9 considering all the possible temperature–time combinations.

2.11 | Response surface methodology modeling

Response surface methodology (RSM) technique was used to determine the optimal temperature–time combination for the heat treatment of TCW using Design Expert 12 (32-bit, Stat-Ease Inc.). Central composite design (CCD) with two independent variables was used for optimization. The face center design lattice was made of eight noncentral and three central points with $\alpha = 1$. The independent variables were temperature (80–95°C) and exposure time (5–15 min). Characteristics of each run were measured using dependent variables, namely pH, TSS, TA, turbidity, phenolic content, relative PPO, relative POD, and OA.

The relationship between independent variables and response was calculated using a second-order polynomial Equation (8).

$$Y = \beta_0 + \sum_{i=1}^{2} \beta_i X_i + \sum_{i=1}^{2} \beta_{ii} X_i X_i + \beta_{12} X_1 X_2, \quad (8)$$

where Y = response, β_0 = constant, β_i = linear coefficient, β_{ii} = squared coefficient, β_{12} = cross-product coefficient, and X_i = real value of the independent variable. These coefficients were calculated using Design Expert (Ver. 12.0.1, Stat-Ease, Inc.) during response surface regression.

The significance of various terms in the model equation was determined (Table 2). Statistical parameters such as *F*-value, *p*-value, R^2, and root mean square error (RMSE) were used to evaluate linear, quadratic, and second-order interaction terms.

2.12 | Enzyme inactivation kinetics

Inactivation kinetics of PPO and POD were studied to understand the relationship between decay in enzyme activity and exposure time. The temperature was kept constant, and samples were treated at various exposure times. Different order reaction equations were derived from the rate law expression, as shown in Equation (9).

$$Rate \propto [A]^n, \quad (9)$$

TABLE 2 ANOVA for quadratic model developed for different parameters of tender coconut water

Source	pH			TSS			Turbidity			Titratable acidity			Relative PPO			Relative POD			Phenolic content			Overall acceptability		
	df	*F*-value	*p*-value	*df*	*F*-value	*p*-value	*df*	*F*-value	*p*-value	*df*	*F*-value	*p*-value	*df*	*F*-value	*p*-value	*df*	*F*-value	*p*-value	*df*	*F*-value	*p*-value	*df*	*F*-value	*p*-value
Model	5	1.75	.2776	2	7.55	.0144	5	32.52	.0008	5	22.21	.0020	5	110.19	<.0001	5	105.43	<.0001	5	22.34	.0020	5	598.53	<.0001
A-temperature	1	0.1775	.6911	1	10.21	.0127	1	92.70	.0002	1	81.41	.0003	1	391.69	<.0001	1	440.60	<.0001	1	61.96	.0005	1	2,190.88	<.0001
B-time	1	0.1775	.6911	1	4.89	.0579	1	51.58	.0008	1	14.83	.0120	1	11.71	.0188	1	21.05	.0059	1	13.98	.0134	1	126.19	<.0001
AB	1	0.1704	.6969				1	14.70	.0122	1	8.79	.0313	1	3.65	.1143	1	6.87	.0470	1	0.6110	.4698	1	1.31	.3035
A^2	1	4.78	.0804				1	2.90	.1496	1	5.10	.0735	1	118.58	.0001	1	50.39	.0009	1	24.52	.0043	1	589.72	<.0001
B^2	1	1.44	.2834				1	0.1311	.7321	1	0.1072	.7566	1	3.78	.1096	1	0.7651	.4218	1	3.32	.1279	1	5.69	.0627
Residual	5			8			5			5			5			5			5			5		
Lack of fit	3			6	18.61	.0519	3	11.66	.0800	3	0.4258	.7567	3			3			3	3.89	.2110	3	6.26	.1408
Pure error	2			2			2			2			2			2			2			2		
Cor total	10			10			10			10			10			10			10			10		

Abbreviations: POD: peroxidase; PPO, polyphenol oxidase; TSS, total soluble solids.

where $[A]$ is the concentration of reacting species and n is the order of the reaction.

Various enzyme inactivation governing equations were fitted using MATLAB online 2020a using the curve fitting application. Data were imported to the MATLAB workspace, and multiple equations were provided as custom equations in the curve fitting application. The fitted models were compared using sum of squares (SSE), R^2, and RMSE values to determine the best fit.

2.13 | Zeroth-, first-, and second-order kinetics

Depending on the concentration of reacting species, different values (0, 1, and 2) were assigned to the order of reaction in Equation (9). The differential equation was solved, and corresponding equations were formulated. Corresponding to the order of equation, zeroth-, first-, and second-order linear equations were obtained and presented as Equations (10)–(12).

$$[A] = -kt + [A_0], \tag{10}$$

$$\frac{[A]}{[A_0]} = e^{-kt}, \tag{11}$$

$$\frac{1}{[A]} = kt + \frac{1}{[A_0]}, \tag{12}$$

where $[A]$ is the residual activity at any time, t, $[A_0]$ is the initial activity, and k is the rate constant (min^{-1}). From the fitted model rate, constant k is determined.

2.14 | Weibull model

This model was used to represent the inactivation mechanism of enzymes. The residual enzyme activity depended on the intensity of treatment or formation of enzyme resistance. In the Weibull model, the concentration terms and time are correlated and expressed in Equation (13).

$$\frac{[A]}{[A_0]} = e^{-kt^n}, \tag{13}$$

where $[A]$ is the residual activity at any time, t, $[A_0]$ is the initial activity, k determines the curve's scale, and n determines the shape of the curve.

3 | RESULTS AND DISCUSSION

3.1 | Temperature distribution profile

The simulation results combined and temperature versus time curves were plotted as shown in Figure 2. The bottle materials such as PE, PP, and PET took 7.18, 18.8, and 11.59 min, respectively, to reach 84°C. Therefore, PE bottles provide a fast-heating rate, which could potentially retain the quality aspects of TCW better than other materials. At the same time, heating TCW under the ambient condition causes the heat gain from the water bath and losses heat to surroundings. This time duration for the gain and loss cycle is expectedly more during slow heating processes, affecting the quality of TCW. During the response surface optimization, 84°C was found to be an optimal condition for heat treatment. Therefore, heat profile analysis was conducted at 84°C to locate one coldest spot and determine the maximum and minimum temperatures, as shown in Figure 3.

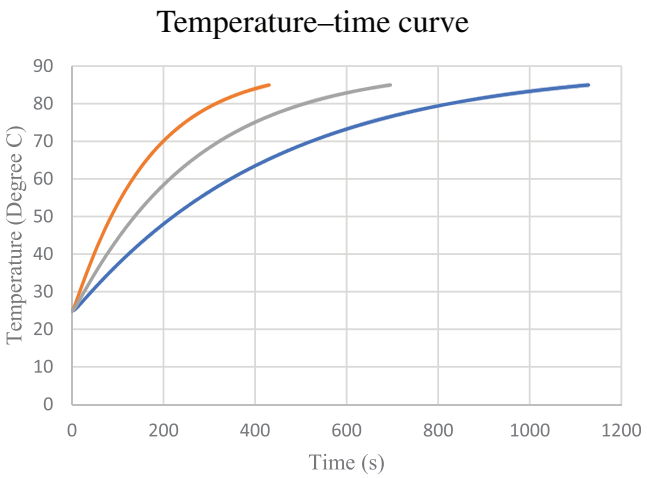

FIGURE 2 Temperature–time response of various materials during heating. ——PP, —— PE, —— PET

From the data, it is evident that PE bottles had the slightest temperature difference between cold and hot spots, thereby exhibiting the uniformity of the heat process. Cold spots were observed at the bottom of the bottle, whereas the hot spots showed peak temperature at the top surface of the liquid with a gradient of a maximum of 4°C. This behavior is due to the motion of liquid from bottom to top during heating by density difference. Also, during practical experiments, it was difficult to estimate these temperature differences using a mercury thermometer or PT-100 probes, which cannot capture the slight variations inside the bottle. Therefore, it is essential to analyze the results of simulation studies and correlate them with practical criteria to decide optimum treatment conditions. Overall, PE was identified as the better-suited material due to its uniform heat distribution and rapid heating. The higher thermal diffusivity and thermal conductivity (6.92×10^{-7} m^2/s) due to the molecular weight and the mobility of molecular chains (Yánez, Rodríguez-Pérez, & Almanza, 2013) are the main reasons for uniform temperature distribution.

3.2 | RSM modeling

The results of the model generated in the heat treatment study are shown in Table 2.

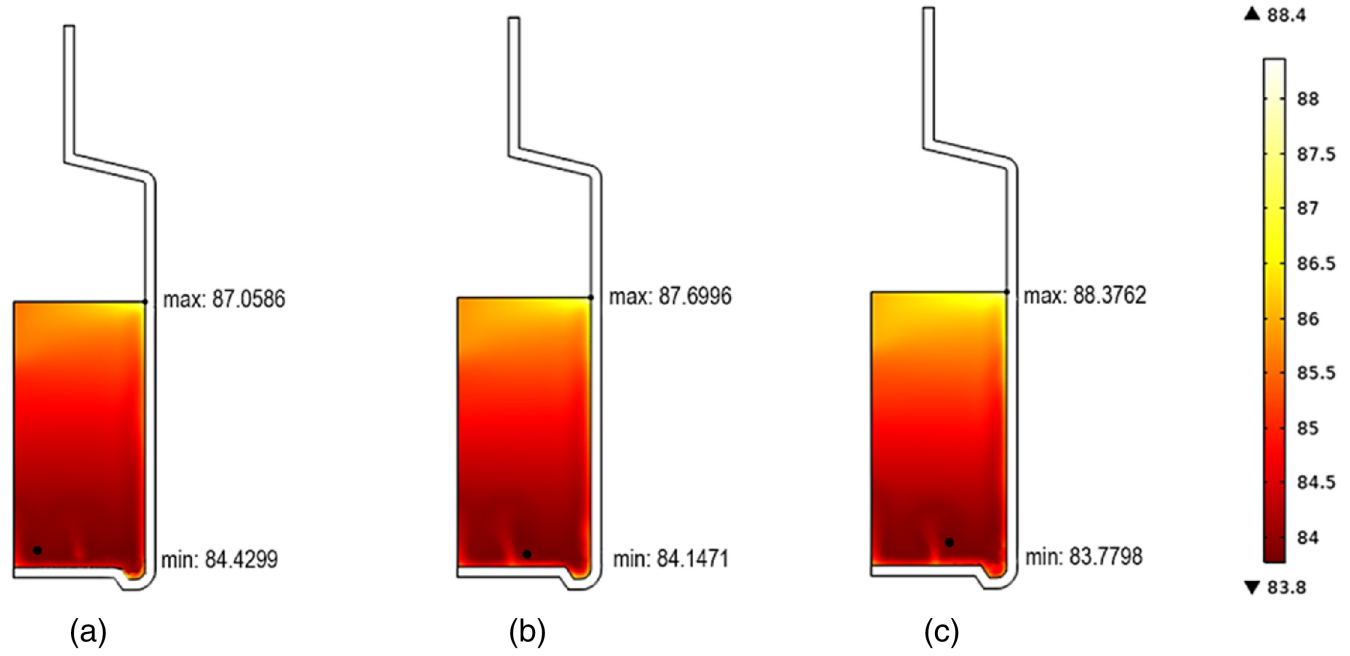

FIGURE 3 Temperature at cold and hot spots of (a) polyethylene, (b) polypropylene, and (c) polyethylene terephthalate

3.3 | Effect of variables on pH

The pH values ranged from 5.43 to 5.57 for various treatments. The lowest pH of TCW was 5.43 for 87.5°C, and 10 min treated sample, whereas the highest pH (5.57) was observed for the treatment of 80°C and 10 min. The fresh samples had a pH of 5.13, which was slightly increased after heat treatment. However, analysis of variance (ANOVA) results have shown that temperature and time do not significantly influence ($p > .05$) the pH of TCW samples after heating. As per FAO guidelines for bottled tender coconut water, the pH range is between 5 and 5.4 (Rolle & FAO, 2007), maintained after heat treatment. The result was similar to Ekasari and Widyarti (2019), with a pH of TCW ranging from 5.49 to 5.64 following heat treatment of 50°C conducted in a gas stove. A quadratic model was selected for pH in terms of independent variables represented in Equation (14).

$$\mathrm{pH} = 5.45737 + 0.00833333 \times A + 0.00833333 \times B - 0.01 \times AB + 0.0665789 \times A^2 + 0.0365789 \times B^2, \quad (14)$$

where A is the temperature and B is the treatment time. Since pH values are nonsignificant, only the constant term in Equation (14) is contributing to the model. As a result, the model had a significantly less R^2 value (0.6537) and adequate precision of 3.16.

3.4 | Effect of variables on TSS

The TSS values ranged from 5.43° to 5.60° Brix for various treatments. Without undergoing the thermal treatment, the fresh sample showed a TSS of 5.45, which increased slightly as the temperature and exposure time increased. It could be attributed to the increase in TSS; a volume reduction of 1.42–10% was observed during heat treatment. Thus, volume reduction caused due to evaporation could increase the TSS of samples. In addition, minor quantities of volatile compounds such as aldehydes, ketones, and esters are present in TCW (Prades, Assa, Dornier, Pain, & Boulanger, 2012). During high-temperature treatment, they also might get evaporated, contributing to an increase in TSS. The range of TSS as per FAO guidelines for bottled tender coconut water is between 5 and 6.5 (Rolle & FAO, 2007), and hence, the TSS observed from this study complies with the guidelines. The statistical analysis suggested that the model was significant and independent variables had their effect on TSS. Therefore, a linear model was selected for TSS in terms of independent variables represented in Equation (15). Since TSS is a parameter that does not require optimization (maximization or minimization), a linear model was chosen for analysis due to better model fit.

$$\mathrm{TSS} = 5.49564 + 0.0541667 \times A + 0.0375 \times B, \quad (15)$$

where A is the temperature and B is the treatment time. The linear term of time with $p < .05$ was found to be the significant term in the model. Indicating that longer treatment time irrespective of the temperature can cause significant changes in TCW. Although the model was found significant with an excellent signal-to-noise ratio (adequate precision = 8.4546), it had low R^2 (0.6537) values due to the scattered residuals. However, the adjusted (0.5672) and predicted R^2 (0.4059) values are less for the response, therefore to predict beyond the experimental range.

3.5 | Effect of variables on turbidity

The turbidity values ranged from 6.173 to 9.246 NTU for various treatments. The fresh TCW sample exhibited turbidity of 6.1 NTU, increasing as the temperature and exposure time increased. Awua, Doe, and Agyare (2011) observed a similar increase in turbidity due to phenolic oxidation, Maillard reaction, and caramelization heat treatment increased turbidity (Tetra Pack, 2019). The high temperature provided during autoclaving and irradiation of TCW also had an increase in turbidity. Therefore, the model was converted to a quadratic model to minimize turbidity, as shown in Equation (16).

$$\text{Turbidity} = 7.59074 + 0.826667 \times A + 0.616667 \times B + 0.40325 \times AB - 0.224842 \times A^2 - 0.478421 \times B^2, \quad (16)$$

where A is the temperature and B is the treatment time. This model has an R^2 value of 0.9702, implying that the data are very closely fitted to Equation (16). However, the adjusted and predicted R^2 ($R^2_{(adj)} = 0.9403$, $R^2_{(pred)} = 0.6995$) lie with a difference greater than 0.2 suggesting that the model has less ability to predict beyond the experimental range. This model also showed a high signal-to-noise ratio (adequate precision = 18.58) greater than 4, which is desirable for a good model (Sharma, Yadav, Mridula, & Gupta, 2016). Also, all the runs were in the acceptable difference in betas (DFBETAS), suggesting no significant influence on coefficients of the formulated equation. However, the DFFITS (difference in fits) shows that the two extreme runs significantly influence the model's fit, supported in Cook's distance plot.

3.6 | Effect of variables on TA

The TA is expressed as mass of malic acid per 100 ml that ranges from 0.0547 to 0.0517%. The highest TA corresponds to 80°C for 5 min treatment time, decreasing as the temperature and treatment time increased. There was a decrease in TA compared with the control sample (TA = 0.079% of malic acid). The model was found significant with p-values <.0001. A quadratic model was used for modeling the response. The B^2 term in the model was eliminated due to the insignificance shown in ANOVA, which significantly improved the $R^2_{(pred)}$ value, making it perform outside of the experiment range. The quadratic model obtained is represented in Equation (17).

$$\text{TA} = 0.0583895 - 0.00136667 \times A - 0.000583333 \times B + 0.00055 \times AB + 0.000526316 \times A^2 + 7.63158e-05 \times B^2, \quad (17)$$

where A is the temperature and B is the treatment time. The model has $R^2 = 0.9569$, which indicates a better fitting model. The adjusted (0.9138) and predicted R^2 values (0.7739) were also in good agreement with a high signal-to-noise ratio (adequate precision = 14.39). Furthermore, one of the central points runs significantly impacted DFFITS and DFBETAS plots, which recorded the most negligible TA value among the central points; however, the model does not significantly lack fit. This is the reason for the high residuals for the run during prediction, which then caused the drop in predicted R^2.

3.7 | Effect of variables on PPO

The PPO inactivation was represented as a relative inactivation rate concerning the control sample. The TCW had a PPO level of 0.97 U/ml and declined when the temperature crossed 80°C. It was observed that the treatment of 87.5°C for 5 min exposure time was able to inactivate the enzymes completely. Also, only 12% inactivation was observed at 80°C for 5 min exposure, usually regarded as the temperature at which PPO inactivation is carried out. Inactivation kinetics of PPO suggested that the inactivation of enzymes started at 70°C (Ioniţă et al., 2017). Generally, PPO reacts with phenolic compounds using them as substrate, causing the appearance of pink color (Matsui et al., 2007; Nokthai et al., 2010). A UPLC-HRMS (ultra-performance liquid chromatography–high-resolution mass spectrometry) analysis conducted by Cunha et al. (2020) found that procyanidin A-type dimer and trimer in the negative ionization mode along with some other unidentified compounds are reasons for the stabilization of anthocyanin pigments causing pink color (Cunha et al., 2020). The high-temperature treatment affects the catalytic behavior of enzymes by destroying the α-helix and β-sheet structures (Murtaza et al., 2018). These change the structure of the active site of the enzyme, thereby inactivating the same.

The relative enzyme reduction ranged from 22 to 95% inactivation; therefore, a square root transformation was performed for a better result. The transformation was suggested in the diagnostics tab of software, based on various matrices used for visualizing the data trend. Also, the sudden decline in PPO activity at 87.5°C will remain an outlier without proper data transformation. The model was found significant with a p-value <.0001 represented by Equation (18).

$$\sqrt{\text{PPO}} = 0.021907 - 0.417444 \times A - 0.0721926 \times B + 0.0493633 \times AB + 0.353481 \times A^2 + 0.0630837 \times B^2, \quad (18)$$

where A is the temperature and B is the treatment time. The analysis obtained a high R^2 (0.9910) which indicates a well-fitted model. Proper outlier treatment allowed for a higher adjusted (0.9820) and predicted R^2 values (0.9225). The particular response also maintained adequate high precision (26.71) though signals dominated the noise. However, since the procedure for PPO determination was dependent on the slope of the absorbance curve, the repeated central points did not have a significant difference up to three decimal points. As a result, the lack of fit of the model was not evaluated for the response. Since the DFBETA values were in the acceptable range, the formulated coefficients of the equations have no bias to runs.

3.8 | Effect of variables on POD inactivation

The POD inactivation was represented as a relative inactivation rate concerning the control sample. Due to the high biological variation of tender coconuts, relative inactivation will be more appropriate than direct readings. Raw TCW had 1.8 U/ml POD activity, which started to decrease on heat treatment. The highest POD activity was measured at 80°C for 5 min treatment time, whereas complete inactivation was achieved at 95°C for 5 min. The observations suggest that PPO compared to POD had higher relative activity for each 5 min increment in treatment time and 7.5°C temperature. Tan et al. (2014) suggested that PPO is more heat resistant than POD during thermal inactivation. However, a contradictory result was obtained for Murasaki-Aliberti, da Silva, Gut, and Tadini (2009). This varying trend may be due to various geographical (Brazil and Malaysia) and biological variations of the samples used in these studies. It was observed that even after complete inactivation of PPO, 2% of POD activity remained at 87.5°C for 10 min. A similar behavior of significant and rapid decline in PPO activity compared to POD activity was observed during ultraviolet treatment on TCW (Augusto, Ibarz, Garvín, & Ibarz, 2015). Complete inactivation was found at 90°C during thermal inactivation for POD extract from tomato (de los Santos et al., 2020), whereas complete inactivation was observed at 95°C for TCW.

The residual versus run plot was used to find outliers, and the software diagnostics used square root transformation. This improved overall R^2 values (0.88–0.99) allowed higher R^2 adjusted (0.0980) and predicted (0.9090), enabling adequately accurate prediction beyond the experimental range. The response obtained a significant model with a p-value <.0001 represented in Equation (19).

$$\sqrt{\text{POD}} = 0.16153 - 0.3698 \times A - 0.0808375 \times B + 0.0565568 \times AB + 0.19246 \times A^2 + 0.023716 \times B^2, \quad (19)$$

where A is the temperature and B is the treatment time. The data set had a higher signal-to-noise ratio (adequate precision = 28.278), enabling proper navigation in the design space. Furthermore, the drop-in POD activity at 87.5°C was having a significant impact on DFFITS and DFBETAS plots, which remained within the acceptable limits. Since POD is calculated from the slope of the absorbance curve, which had only negligible variations and the lack of fit of the model was not calculated.

3.9 | Effect of variables on phenolic content

The phenolic content was represented in mg GAE per liter, ranging from 38.64 to 44.42 mg GAE/L. The raw TCW has a phenolic content of 49.20 mg GAE/L, which slightly decreased heat treatment. The same trend was observed by Sanganamoni, Mallesh, Vandana, and Srinivasa Rao (2017); this may be due to the production of free radicals that may degrade polyphenols by oxidizing them (Rajashri et al., 2020).

A quadratic model was selected for the response with p-value = .0010, thus rendering a significant model. The variation of phenolic content with independent variables is represented by Equation (20).

$$\text{Phenolic content} = 44.2321 - 2.035 \times A - 0.0966667 \times B - 0.2475 \times AB - 1.97026 \times A^2 - 0.725263 \times B^2, \quad (20)$$

where A is the temperature and B is the treatment time. The model was a good fit for the quadratic equation with $R^2 = 0.9572$. Although the difference in R^2 adjusted (0.9143) and predicted (0.7226) are 0.2, which may not give accurate predictions beyond the experimental range. The data, however, had adequate precision (13.2272), suggesting a higher signal-to-noise ratio. Similar to turbidity, the extreme runs had an influence on DFFITS values for phenolic content data. However, overall DFBETAS, cook distance, and residuals during predictions were acceptable limits with an insignificant lack of fit.

3.10 | Effect of processing variables on sensory evaluation

The Hedonic scale rating evaluated aroma, fermentation, freshness, sweetness, burnt, off-flavor, color, and OA. The sensory evaluation results are shown in Figure 4.

When exposed to a higher temperature, the samples develop off-flavor, and most of the other qualities are also found to have a detrimental effect. The color development for samples S6, S7, S8, and S9 is mild yellow shades. This may be due to nonenzymatic browning, namely Maillard reaction and caramelization (Tetra Pack, 2019). The panel also reported that cooked flavor started appearing for the TCW samples at 87.5 and 90°C, decreasing OA. The off-flavor might be due to the evaporation of TCW volatile components (aldehydes, ketones, and esters) (Prades et al., 2012).

Similarly, caramelization and Maillard reaction in strawberry products also developed an undesired burnt smell during thermal treatment at 60–90°C (Ozcan, Tamer, & Çopur, 2018). The trend shows that after S6, the sensory qualities start to degrade rapidly; therefore, temperatures below 87.5°C should be selected for optimization. The heat treatment influences the sensory quality of the product, but since it is essential for enzyme inactivation, treatment with minimal quality loss is chosen.

Overall acceptability determined by the predetermined panel ranged from 4.33 to 7.83. The model was found significant with a p-value <.0001. A quadratic model was selected for the response represented by Equation (21).

$$\text{OA}^{2.59} = 174.49 - 65.3694 \times A - 16.4146 \times B + 4.19774 \times AB - 47.5376 \times A^2 - 5.31022 \times B^2, \quad (21)$$

where A is the temperature and B is the treatment time. The model had an $R^2 = 0.9983$, which is a good data fit. Maintaining an adequate

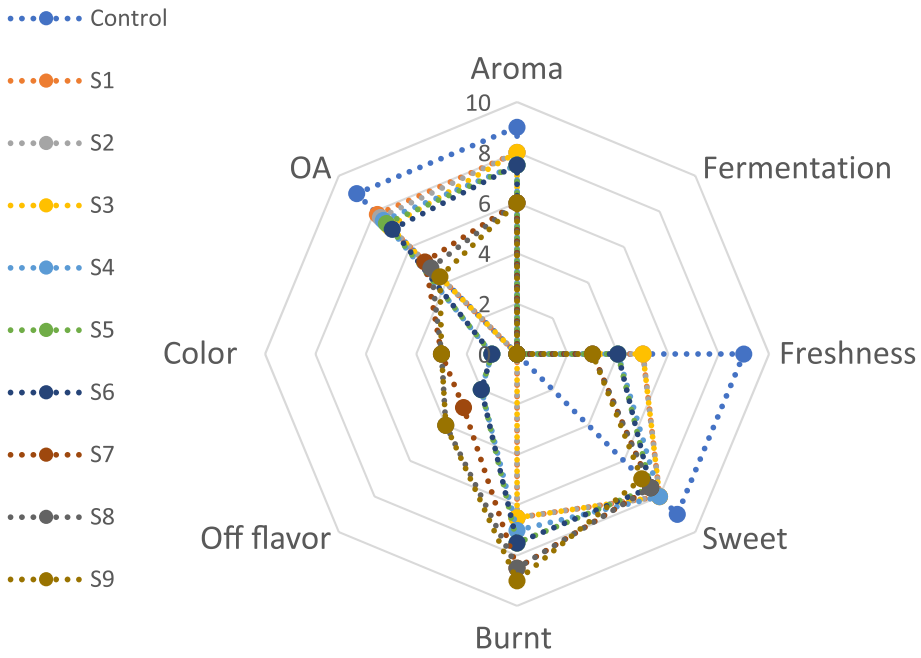

FIGURE 4 Radar representation of sensory evaluation of heat-treated samples

high precision (64.1661) reduces the data noise to a significant amount. The model exhibited R^2 adjusted (0.9967) and predicted (0.9838), indicating its good prediction capacity beyond the experimental range.

3.11 | Optimization of processing conditions

The independent variables were optimized using Design Expert (Ver.12.0.1., Stat-Ease, Inc.). Among the eight responses (Figure 5) recorded, five important parameters were taken for optimization. The pH was found nonsignificant ($p > .05$) and not considered in the optimization. Similarly, TSS response was within preferred FAO limits, therefore, not considered for optimization. TA had a good model fit, but the values were acceptable limits, thus avoiding optimization. Optimization was carried out by setting a condition, lower and higher limit, and importance for each response, as shown in Table 3.

The importance of 4 was given to the relative activity of PPO and POD and OA since these responses directly influence the quality of TCW. Nevertheless, a higher phenolic content is considered an additional benefit due to its health benefits (Ozcan et al., 2018). Therefore, the response for the relative activity of PPO and POD was given a weight of 0.5 since 95.00% inactivation of PPO, and 89% inactivation of POD was found at 87.5°C at 5 min exposure time. The same approach was suggested by Chourio, Salais-Fierro, Mehmood, Martinez-Monteagudo, and Saldaña (2018), where greater than 90% inactivation was a recommended condition for designing a process that extends shelf life. Furthermore, this approach was selected since a prolonged heat exposure can cause a nonenzymatic browning reaction, namely Maillard reaction and caramelization. This is due to free amino acids and reducing sugars in TCW (Tan et al., 2014). The optimized conditions obtained as per set criteria are shown in Table 4.

The temperature optimized was found reasonable with good desirability of 0.926. The optimized results agreed with Gunathunga, Abeywickrema, and Navaratne (2018), where heating at 85°C maintained high organoleptic properties. Optimized parameters were then validated through experiment, as shown in Table 4. The values were nearly equal to predicted once, thus reconfirming the validity of the model.

3.12 | Enzyme inactivation kinetics of PPO and POD

To find the best fit, enzyme inactivation kinetics was studied for zeroth-, first-, second-order, and Weibull models. A kinetic study was conducted at 80°C for 5, 10, 15, 20, 25, and 30 min to obtain various inactivation levels. The decimal reduction time and half-life of PPO and POD were calculated according to first-order kinetics. The fitted models were compared with SSE, R^2, and RMSE values, as shown in Table 5.

The data analysis showed that the Weibull model was suitable for explaining the enzyme kinetics of both PPO and POD during the heating of coconut water. A higher value of regression coefficient (R^2) and low SSE and RMSE indicate the model's ability to explain the kinetics of PPO and POD. Furthermore, a study conducted by Chourio et al. (2018) and Ma et al. (2019) tested pressure-assisted thermal processing (maximum temperature: 90°C) of TCW and found the

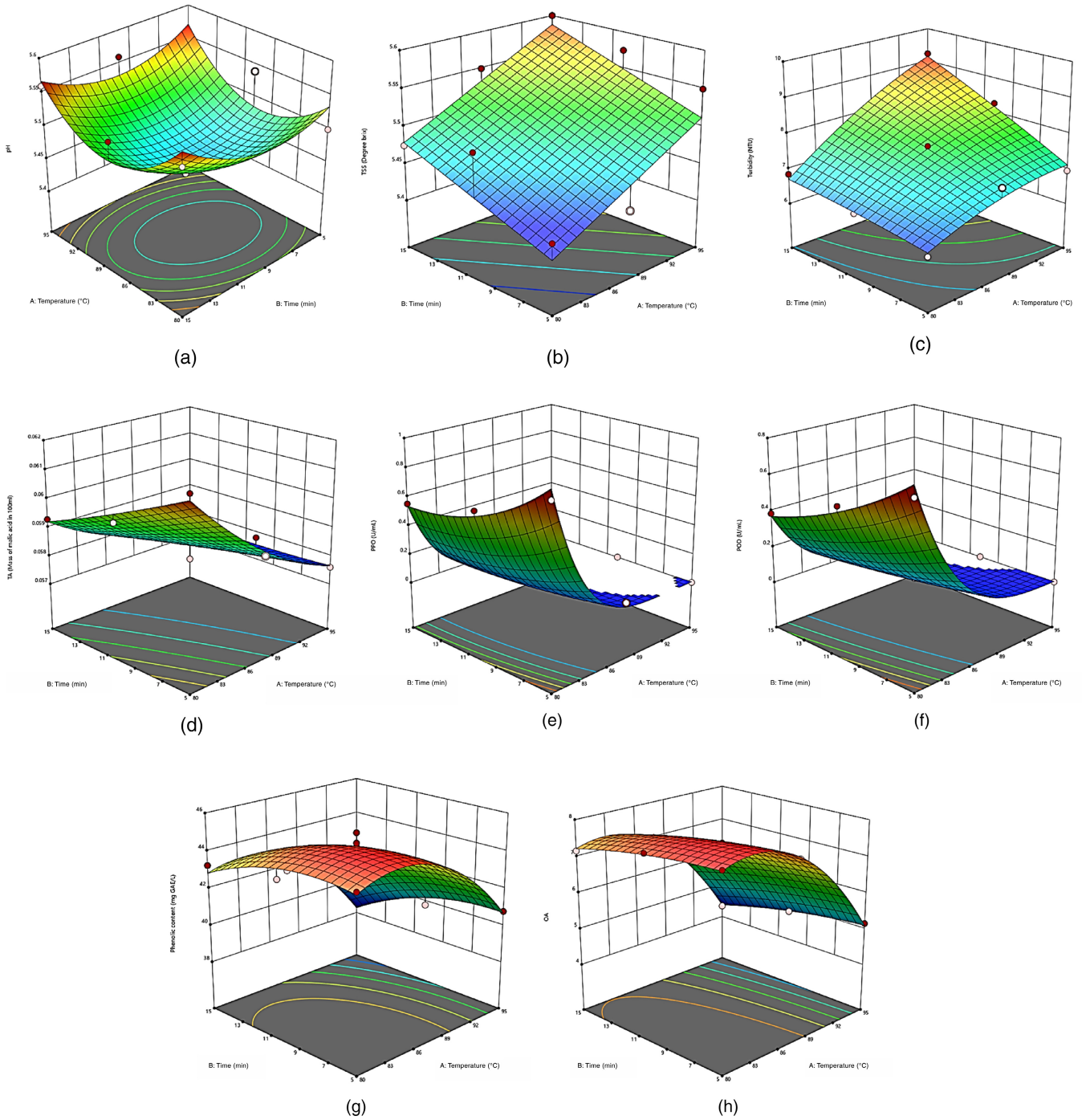

FIGURE 5 Response surface plots illustrating effect of temperature and time on (a) pH, (b) total soluble solids, (c) turbidity, (d) titratable acidity, (e) polyphenol oxidase, (f) peroxidase, (g) phenolic content, and (h) overall acceptability

TABLE 3 Optimization conditions and corresponding parameters for RSM

Responses	Condition	Lower limit	Upper limit	Importance
Turbidity (NTU)	Minimize	6.1730	9.2460	3
Relative activity of PPO (%)	Minimize	0	0.8889	4
Relative activity of POD (%)	Minimize	0	0.7222	4
Total phenolic content (mg of GAE/L)	Maximize	38.6400	44.4400	3
Overall acceptability	Maximize	4.3333	7.8333	4

Abbreviations: GAE, gallic acid equivalent; POD, peroxidase; PPO, polyphenol oxidase; RSM, response surface methodology; TSS, total soluble solids.

TABLE 4 Predicted and experimental values for tender coconut water processed by thermal treatment

Values	Temperature (°C)	Time (min)	pH	TSS (°Brix)	Turbidity (NTU)	Titratable acidity (% of malic acid)	Relative PPO (%)	Relative POD (%)	Phenolic content (mg of GAE/L)	Overall acceptability	Desirability
Predicted	83.84	5	5.39	5.44	6.67	0.06	0.105	0.095	44.83	7.80	0.926
Expire mental	84	5	5.4	5.52	7.10	0.06	0.099	0.093	44.71	8.00	—

Abbreviations: GAE, gallic acid equivalent; POD, peroxidase; PPO, polyphenol oxidase.

TABLE 5 Curve fitting data for PPO and POD

Model	Constants	SSE	R^2	RMSE
Kinetic curve fitting data for PPO				
Zeroth order	$k = 0.01765$	0.0108	0.9353	0.0465
First order	$k = 0.03064$	0.0217	0.9168	0.0659
Second order	$k = 0.06137$	0.2491	0.9156	0.2232
Weibull	$k = 0.0112$, $n = 1.336$	0.0114	0.9562	0.0535
Kinetic curve fitting data for POD				
Zeroth order	$k = 0.0379$	0.1096	0.6558	0.1480
First order	$k = 0.03481$	0.0347	0.8909	0.0833
Second order	$k = 0.04603$	0.1708	0.8992	0.1848
Weibull	$k = 0.01175$, $n = 1.366$	0.0205	0.9355	0.0716

Abbreviations: POD, peroxidase; PPO, polyphenol oxidase; RMSE, root mean square error; SSE, sum of squares.

enzyme kinetic study resulting in a good fit of Weibull model. However, the kinetics study was not extended to 87.5°C since complete inactivation of PPO was detected at 5 min and POD at 20 min, therefore reduced the number of points for a proper kinetics study.

4 | CONCLUSION

Optimization of temperature and processing time would enhance the shelf life of the TCW. The selection of proper packaging material could preserve the nutritional profile of the TCW. The temperature distribution studies indicated that PE bottles have better uniformity while heating along with lesser exposure time. It was found that the thermal treatment at 83.8°C for 5 min was able to inactivate the enzymes in fresh TCW. It is worth noting that the optimized treatment conditions for TCW conserved most of the sensory properties. Heat treatment at very high temperatures such as 95 and 120°C were causing Millard reaction and the destruction of inherent flavor. The optimized treatment was able to address these challenges to a great extent.

ACKNOWLEDGMENTS

The current study was funded by AICRP on PHET, Indian Council of Agricultural Research, New Delhi, India.

CONFLICT OF INTEREST

The authors declare no potential conflict of interest.

AUTHOR CONTRIBUTIONS

V. Prithviraj: Data curation; methodology; software; validation; writing – original draft. **Ravi Pandiselvam:** Conceptualization; investigation; methodology; resources; validation; writing – original draft; writing – review and editing. **S V Ramesh:** Methodology; resources; writing – review and editing. **Shameena Beegum P. P.:** Investigation; writing – review and editing. **Anjineyulu Kothakota:** Methodology; resources; writing – review and editing. **Amin Mousavi khaneghah:** Resources; writing – review and editing.

ETHICS STATEMENT

There was no need for ethics approval for the present research.

DATA AVAILABILITY STATEMENT

The data that support the findings of this study are available on request from the corresponding author.

ORCID

Ravi Pandiselvam https://orcid.org/0000-0003-0996-8328
M. R. Manikantan https://orcid.org/0000-0002-0170-7150
P. P. Shameena Beegum https://orcid.org/0000-0003-4391-2643
Anjineyulu Kothakota https://orcid.org/0000-0002-5972-3356
Amin Mousavi Khaneghah https://orcid.org/0000-0001-5769-0004

REFERENCES

Augusto, P. E. D., Ibarz, R., Garvín, A., & Ibarz, A. (2015). Peroxidase (POD) and polyphenol oxidase (PPO) photo-inactivation in a coconut water

model solution using ultraviolet (UV). *Food Research International*, *74*, 151–159. https://doi.org/10.1016/j.foodres.2015.04.046

Awua, A. K., Doe, E. D., & Agyare, R. (2011). Exploring the influence of sterilisation and storage on some physicochemical properties of coconut (*Cocos nucifera* L.) water. *BMC Research Notes*, *4*(1), 451. https://doi.org/10.1186/1756-0500-4-451

Camargo Prado, F., de Dea Lindner, J., Inaba, J., Thomaz-Soccol, V., Kaur Brar, S., & Soccol, C. R. (2015). Development and evaluation of a fermented coconut water beverage with potential health benefits. *Journal of Functional Foods*, *12*, 489–497. https://doi.org/10.1016/j.jff.2014.12.020

Campbell-Falck, D., Thomas, T., Falck, T. M., Tutuo, N., & Clem, K. (2000). The intravenous use of coconut water. *American Journal of Emergency Medicine*, *18*(1), 108–111. https://doi.org/10.1016/S0735-6757(00)90062-7

Chourio, A. M., Salais-Fierro, F., Mehmood, Z., Martinez-Monteagudo, S. I., & Saldaña, M. D. A. (2018). Inactivation of peroxidase and polyphenoloxidase in coconut water using pressure-assisted thermal processing. *Innovative Food Science and Emerging Technologies.*, *49*, 41–50. https://doi.org/10.1016/j.ifset.2018.07.014

Cunha, A. G., Alves Filho, E. G., Silva, L. M. A., Ribeiro, P. R. V., Rodrigues, T. H. S., Brito, E. S., & Miranda, M. R. A. . (2020). Chemical composition of thermally processed coconut water evaluated by GC–MS, UPLC-HRMS, and NMR. *Food Chemistry*, *324*, 126874. https://doi.org/10.1016/j.foodchem.2020.126874

de los Santos, M. B., Jacobi, S. S., Miñarro, M. C. A., Balsalobre, J. A. P., Guillén, A. A., & Gorbe, M. I. F. (2020). Kinetic characterization, thermal and pH inactivation study of peroxidase and pectin methylesterase from tomato (*Solanum betaceum*). *Food Science and Technology*, *40*(June), 273–279. https://doi.org/10.1590/fst.09419

Ekasari, C. P., & Widyarti, S. (2019). The physicochemical properties comparison of the natural coconut water and the packaging coconut water. *IOP Conference Series: Earth and Environmental Science*, *391*(1), 012021. https://doi.org/10.1088/1755-1315/391/1/012021

Gunathunga, C., Abeywickrema, S., & Navaratne, S. (2018). Preservation of tender coconut (*Cocos nucifera* L.) water by heat and UV-C treatments. *International Journal of Food Sciences and Nutrition*, *3*(3), 15–19.

Ioniță, E., Gurgu, L., Aprodu, I., Stănciuc, N., Dalmadi, I., Bahrim, G., & Râpeanu, G. (2017). Characterization, purification, and temperature/pressure stability of polyphenol oxidase extracted from plums (*Prunus domestica*). *Process Biochemistry*, *56*, 177–185. https://doi.org/10.1016/j.procbio.2017.02.014

Ma, Y., Xu, L., Wang, S., Xu, Z., Liao, X., & Cheng, Y. (2019). Comparison of the quality attributes of coconut waters by high-pressure processing and high-temperature short time during the refrigerated storage. *Food Science and Nutrition*, *7*(4), 1512–1519. https://doi.org/10.1002/fsn3.997

Matsui, K. N., Granado, L. M., de Oliveira, P. V., & Tadini, C. C. (2007). Peroxidase and polyphenol oxidase thermal inactivation by microwaves in green coconut water simulated solutions. *LWT—Food Science and Technology*, *40*(5), 852–859. https://doi.org/10.1016/j.lwt.2006.03.019

Mosqueda-Melgar, J., Raybaudi-Massilia, R. M., & Martín-Belloso, O. (2012). Microbiological shelf life and sensory evaluation of fruit juices treated by high-intensity pulsed electric fields and antimicrobials. *Food and Bioproducts Processing*, *90*(2), 205–214.

Murasaki-Aliberti, N. D. C., da Silva, R. M. S., Gut, J. A. W., & Tadini, C. C. (2009). Thermal inactivation of polyphenoloxidase and peroxidase in green coconut (Cocos nucifera) water. *International Journal of Food Science and Technology*, *44*(12), 2662–2668. https://doi.org/10.1111/j.1365-2621.2009.02100.x

Murtaza, A., Muhammad, Z., Iqbal, A., Ramzan, R., Liu, Y., Pan, S., & Hu, W. (2018). Aggregation and conformational changes in native and thermally treated polyphenol oxidase from apple juice (*Malus domestica*). *Frontiers in Chemistry*, *6*(JUN), 1–10. https://doi.org/10.3389/fchem.2018.00203

Naik, M., Sunil, C. K., Rawson, A., & Venkatachalapathy, N. (2020). Tender coconut water: a review on recent advances in processing and preservation. *Food Reviews International*, 1–22. https://doi.org/10.1080/87559129.2020.1785489

Nokthai, P., Lee, V. S., & Shank, L. (2010). Molecular modeling of peroxidase and polyphenol oxidase: Substrate specificity and active site comparison. *International Journal of Molecular Sciences*, *11*(9), 3266–3276. https://doi.org/10.3390/ijms11093266

Olufunmi, O., Daniel, A., & Efem, R. (2020). Antimicrobial activity of coconut water, oil and palm kernel oils extracted from coconut and palm kernel on some plasmid-mediated multi-drug resistant organisms associated with food spoilage. *African Journal of Microbiology Research*, *14*(7), 366–373. https://doi.org/10.5897/AJMR2020.9363

Ozcan Sinir, G., Tamer, C., & Çopur, Ö. (2018) Effect of several food processing methods on volatile composition of strawberry. pp. 179–182. https://doi.org/10.3217/978-3-85125-593-5-40.

Pandiselvam, R., Manikantan, M. R., Balasubramanian, D., Beegum, P. P. S., Mathew, A. C., Ramesh, S. V., … Niral, V. (2020). Mechanical properties of tender coconut (*Cocos nucifera* L.): Implications for the design of processing machineries. *Journal of Food Process Engineering*, *43*(2), 1–8. https://doi.org/10.1111/jfpe.13349

Pandiselvam, R., Manikantan, M. R., Sunoj, S., Sreejith, S., & Beegum, S. (2019). Modeling of coconut milk residue incorporated rice-corn extrudates properties using multiple linear regression and artificial neural network. *Journal of Food Process Engineering*, *42*(2), 1–10. https://doi.org/10.1111/jfpe.12981

Porto, E., Alves Filho, E. G., Silva, L. M. A., Fonteles, T. V., do Nascimento, R. B. R., Fernandes, F. A. N., … Rodrigues, S. (2020). Ozone and plasma processing effect on green coconut water. *Food Research International*, *131*, 109000. https://doi.org/10.1016/j.foodres.2020.109000

Prades, A., Assa, R. R. A., Dornier, M., Pain, J. P., & Boulanger, R. (2012). Characterisation of the volatile profile of coconut water from five varieties using an optimised HS-SPME-GC analysis. *Journal of the Science of Food and Agriculture*, *92*(12), 2471–2478. https://doi.org/10.1002/jsfa.5655

Pravitha, M., Manikantan, M. R., Kumar, V. A., Beegum, S., & Pandiselvam, R. (2021). Optimization of process parameters for the production of jaggery infused osmo-dehydrated coconut chips. *LWT*, *146*, 111441. https://doi.org/10.1016/j.lwt.2021.111441

Rajashri, K., Roopa, B. S., Negi, P. S., & Rastogi, N. K. (2020). Effect of ozone and ultrasound treatments on polyphenol content, browning enzyme activities, and shelf life of tender coconut water. *Journal of Food Processing and Preservation*, *44*(3), 1–11. https://doi.org/10.1111/jfpp.14363

Rolle, R. S., & FAO (2007). Good practice for the small-scale production of bottled coconut water. In *Food and Agriculture Organization of the United Nations (agricultural and food engineering training and resource materials)*. Rome, Italy: FAO. Retrieved from https://books.google.co.in/books?id=ZUduUKj_tZgC

Sanganamoni, S., Mallesh, S., Vandana, K., & Srinivasa Rao, P. (2017). Thermal treatment of tender coconut water – Enzyme inactivation and biochemical characterization. *International Journal of Current Microbiology and Applied Sciences*, *6*(5), 2919–2931. https://doi.org/10.20546/ijcmas.2017.605.331

Segura-Badilla, O., Lazcano-Hernández, M., Kammar-García, A., Vera-López, O., Aguilar-Alonso, P., Ramírez-Calixto, J., & Navarro-Cruz, A. R. (2020). Use of coconut water (*Cocus nucifera* L) for the development of a symbiotic functional drink. *Heliyon*, *6*(3), e03653. https://doi.org/10.1016/j.heliyon.2020.e03653

Sharma, M., Yadav, D. N., Mridula, D., & Gupta, R. K. (2016). Protein enriched multigrain expanded snack: Optimization of extrusion variables. *Proceedings of the National Academy of Sciences India Section B: Biological Sciences*, *86*(4), 911–920. https://doi.org/10.1007/s40011-015-0546-5

Singleton, V. L., Orthofer, R., & Lamuela-Raventós, R. M. (1999). Analysis of total phenols and other oxidation substrates and antioxidants by means of Folin-Ciocalteu reagent. In *Lipids* (pp. 152–178). https://doi.org/10.1016/S0076-6879(99)99017-1

Tan, T. C., Cheng, L. H., Bhat, R., Rusul, G., & Easa, A. M. (2014). Composition, physicochemical properties and thermal inactivation kinetics of polyphenol oxidase and peroxidase from coconut (*Cocos nucifera*) water obtained from immature, mature and overly-mature coconut. *Food Chemistry*, *142*, 121–128. https://doi.org/10.1016/j.foodchem.2013.07.040

Tan, T. C., Cheng, L.-H., Bhat, R., Rusul, G., & Mat Easa, A. (2015). Effectiveness of ascorbic acid and sodium metabisulfite as anti-browning agent and antioxidant on green coconut water (*Cocos nucifera*) subjected to elevated thermal processing. *International Food Research Journal*, *22*(2), 631–637.

Tetra Pack. (2019). *Coconut handbook (composition)* (pp. 1–16). Switzerland: Tetra Pak International. Retrieved from https://coconuthandbook.tetrapak.com/

Thimmaiah, S. K. (1999). *Standard methods of biochemical analysis*. New Delhi: Kalyani Publishers. Retrieved from https://books.google.co.in/books?id=U5N4uQEACAAJ

Vamos-Vigyázó, L. (1981). Polyphenol oxidase and peroxidase in fruits and vegetables. *Critical Reviews in Food Science and Nutrition*, *15*(1), 49–127. https://doi.org/10.1080/10408398109527312

Yánez, G., Rodríguez-Pérez, M. A., & Almanza, O. A. (2013). LDPE and PP thermal diffusivity in molten state. *Ingenieria e Investigacion*, *33*(2), 5–8.

Yong, J. W. H., Ge, L., Ng, Y. F., & Tan, S. N. (2009). The chemical composition and biological properties of coconut (*Cocos nucifera* L.) water. *Molecules*, *14*(12), 5144–5164. https://doi.org/10.3390/molecules14125144

How to cite this article: Prithviraj, V., Pandiselvam, R., Manikantan, M. R., Ramesh, S. V., Shameena Beegum, P. P., Kothakota, A., & Mousavi Khaneghah, A. (2022). Transient computer simulation of the temperature profile in different packaging materials: An optimization of thermal treatment of tender coconut water. *Journal of Food Process Engineering*, *45*(10), e13958. https://doi.org/10.1111/jfpe.13958